

Research Journal of Pharmaceutical, Biological and Chemical Sciences

Evaluation of the Testicular Alterations Induced By Silver Nanoparticles in Male Mice: Biochemical, Histological and Ultrastructural Studies

Azza A. Attia*

Zoology Department, Faculty of Science, Alexandria University, Alexandria, Egypt.

ABSTRACT

Despite of many benefits of nanoparticles induced, their increasing usage raises concern about the consequences and health threats that it might bring to humans. So, the current study evaluated the testicular defects after i.p. injection of silver nanoparticles (AgNPs). Male mice, weighing 31-34 g, and of 3 months old were randomly assigned into three groups with respect to concentration of nanoparticles (100, 500 and 1000 mg/kg) for 28 days. Control animals received saline solution as a vehicle. Sperm aspects, oxidative stress, testosterone assay and the testicular histopathology were performed. Results obtained no significant differences in body weight, testes and epididymes weights in all treatments, compared to the control. Silver nanoparticles deteriorated reproductive function of male mice by reduction daily sperm production, viability, progressive sperm motility, and increased sperm DNA integrity and sperm shape abnormalities. All these could affect the fertility. High concentrations (500 & 1000 mg/kg) of AgNPs induced reduction in testosterone hormone, reduced the activity of superoxide dismutase, and increased the level of lipid peroxidation. Histologically, high concentrations of AgNPs caused some disruption in the testicular architecture, testicular atrophy, sloughing and detachment the spermatogenic epithelium. Ultrastructurally, there was an increase in the intercellular spaces between spermatogenic cells, and a considerable degree of deformation in the acrosomal sheath. In conclusion, AgNPs could impair stability of sperm chromatin and stimulated oxidative damage, resulting in the disruption of spermatogenesis at any stage of cell differentiation.

Keywords: Silver nanoparticles, testis, testosterone, oxidative stress, spermatozoa.

**Corresponding author*

INTRODUCTION

With the increasing utilization of nanoparticles (NP), people have a greater opportunity to be exposed to nanoparticles through the occupational environment and consumer products in daily life. Nanoparticles are materials with at least one dimension ≤ 100 nm. They have very specific chemical and physical characteristics of size, shape and large surface-to-volume ratio results in unique characteristics compared to their corresponding bulk materials [1]. These properties facilitate its medical and biological applications.

Despite of many benefits that nanoparticles bring to the society, e.g. in drug delivery systems, medical devices, food products, cosmetics, etc., their increasing usage raises concern about the consequences and health threats that it might bring to humans. These particles can enter the body of an organism through various routes such as dermal, oral and respiratory tract to other parts of the body [2]. Once entered the body, NPs are absorbed and translocated to different organs through the circulatory and lymphatic system [3].

Nanotoxicology refers to the study of the interactions of nanostructures with biological systems with an emphasis on elucidating the relationship between the physical and chemical properties of nanostructures with induction of toxic biological responses [4][5]. Hubbs *et al.* [6] explained that size (and hence the surface/mass ratio) has been considered as the most important factor for the toxicity of NPs, while small particle size does not necessarily lead to better uptake and hence increased toxicity [7].

In vivo, studies showed that these materials may have systemic complications such as weight loss and inflammation [8]. Song *et al.* [9] reported that metal nanoparticles –induced micronuclei and oxidative DNA damage in mice. Roy *et al.* [2] explained that nanoparticles toxicity is compellingly related to oxidative stress, alteration of calcium homeostasis, gene expression, pro-inflammatory responses and cellular signaling events. Among these detrimental substances are silver nanoparticles (AgNPs), which have become one of the most commonly used nanomaterials in consumer products mostly due to its antibacterial properties [10].

Silver nanoparticles are found in cosmetics and used in food packaging [5], medical devices and bandages [11], clothing and washing machines [12], dental restoration material [13] and water treatment facilities [14]. Also, they are used in many domains, such as some imaging and therapeutic purposes, medical implants, catheters, wound dressings and the treatment of burns [15].

Many investigators explained that silver nanoparticles can be accumulated and redistributed between various organs, leading to changes in blood biochemical parameters and inflammation [8][16]. Several studies described the effects of subchronic oral or inhalation toxicity of silver nanoparticles in rodents [17][18]. In these studies, the accumulation of silver was observed in the blood and all tested organs, including the liver, spleen, kidneys, thymus, lungs, heart, brain, and testes. *In vivo* studies have shown that AgNPs are related to injuries to the brain, liver, and lung [19].

Silver nanoparticles can cause cytotoxicity *in vitro* on macrophages and generate free radical production inducing DNA damage [20], decrease mitochondrial function [21], disturb cell cycle progression [22], and depress cellular proliferation [23]. Some reports showed that AgNPs induce apoptosis, necrosis and induce changes in the gene expression, especially in the oxidative stress related genes [24].

In vitro studies demonstrated that AgNPs are cytotoxic by their effect on cellular metabolism and membrane integrity, and inhibit embryonic stem cell differentiation [25].

While there are some reports of AgNPs affecting complex organisms, their effects on reproduction and development have been largely under studied. Silver nanoparticles are concern for male fertility because they have been found to reach the testes after administration [16-18].

Different studies found that AgNPs exposure resulted in morphological abnormalities in a variety of mammalian cell types [4], apoptosis in *Drosophila* larvae [26] and an increase in malformations in fish [27][28]. Li *et al.* [29] showed that AgNPs induced apoptosis in mouse embryos at the blastocyst stage, reduction of implantation frequency and delay in post-implantation development of embryos. Philbrook *et al.* [30] showed that administration of AgNPs to the pregnant CD-1 mice resulted in the reduced fetus viability.

Gromadzka-Ostrowska *et al.* [31] investigated the acute effects of intravenously administration of a single bolus dose of AgNPs on the sperm count, frequency of abnormal spermatozoa, germ cell DNA damage in sperm cells and testis morphometry in the male Wistar rats. Asare *et al.* [32] studied the cytotoxic and genotoxic effects of silver nanoparticles in testicular cells.

Nanosilver particles can interact with membrane proteins and activate signaling pathways, leading to inhibition of cell proliferation [27]. The nanosilver particles can also enter the cell through diffusion or endocytosis to cause mitochondrial dysfunction, generation of reactive oxygen species (ROS), leading to damage to proteins and nucleic acids inside the cell, and finally inhibition cell proliferation [33]. Asharani *et al.* [27] suggested that the disruption of the mitochondrial respiratory chain by nanosilver increases ROS production and interruption of ATP synthesis, thus leading to DNA damage.

Oxidative stress is known to play a crucial role in the aetiology of defective sperm function via mechanisms involving the induction of peroxidative damage to the plasma membrane [34]. The main cellular components susceptible to damage by free radicals are lipids (peroxidation of unsaturated fatty acids in cell membrane) and proteins (denaturation); this in turn can impair cellular structure and function [35].

McShan *et al.* [36] made a review summarized recent advances about the molecular mechanism of nanosilver toxicity. They explained that the toxicity is due to that the surface of

nanosilver can easily be oxidized by O₂ and other molecules in the environmental and biological systems leading to the release of Ag⁺, a known toxic ion. Nanosilver has been shown to penetrate the cell and become internalized. Thus, nanosilver often acts as a source of Ag inside the cell.

Ahamed *et al.* [37] showed that NPs are capable of binding to cells as well as macromolecules like proteins and DNA, leading to alterations in DNA integrity or affecting its synthesis, resulting in formation of mutant or tumorigenic cells. When such processes concern germ line cells, the result may be altered spermatogenesis and fertility, subsequently affecting the reproduction rate and health of the offspring [38].

Although some studies have reported adverse effects of silver nanoparticles on rodent testes as observed by the light microscope, detailed analysis of the morphological effects by the electron microscope has not been reported. Therefore, the present study investigated the effects of intraperitoneally injection of AgNPs at different concentrations on sperm manifestation including count, motility, morphology and viability. Also, biochemical, histological and detailed TEM observations of mouse testes after exposure to these particles were carried out.

MATERIALS AND METHODS

Materials

Characterization of silver nanoparticles (AgNPs)

Silver nanoparticles were provided by the Biophysical Department, Medical Research Institute, Alexandria University, Egypt. The particles were prepared and synthesized by the seeding method (the chemical reduction method) as a suspension of citrate-coated AgNPs [39]. Using the TEM, 90% of the particles were spheres in shape, having smooth surfaces; low level of agglomeration or adhesion, high level of uniformity, and their sizes were ranged from 21 - 41 nm.

Animals and treatments

Forty sexual matured male mice, 3 months old, weighing 31-34 g, were obtained from Faculty of Agriculture, Alexandria University, Alexandria, Egypt. They were housed in polypropylene cages (maximum of 4 mice per cage) in controlled temperature (23 ± 2 °C) and relative humidity (55 ± 5%), with a 12-h light/12-h dark cycle. Animals were fed pellets of a commercial rodent diet and tap water was available *ad libitum* throughout the study. All animals were cared for in accordance with the internationally accepted guidelines for the Care and Use of Laboratory Animals [40]. After two weeks of acclimatization, and according to the approximately equal mean body weight, the animals were assigned to one control and three experimental groups (10 mice each). Experimental mice were injected intraperitoneally with

the prepared AgNPs (dissolved in saline solution) at concentrations of 100, 500 and 1000 mg/kg (dissolved in saline solution) for 28 days [41]. The control animals received saline solution.

Methods

Toxicological assessment of nanosilver

During the time of dosing (28 days), all the experimental mice were inspected for clinical signs of toxicity, which were included: the emotion (excitability, aggressiveness) and autonomous functions (diarrhea, diuresis, salivation) and also mortality.

Body and organs weight

The body weight of each mouse was recorded on day 0 (initial) prior to dosing, and at the end of experiment, all experimental mice and the controls were sacrificed; the reproductive organs (testes and epididymis) were removed, stripped from fatty tissues, blotted, examined macroscopically and weighed. The organs weight coefficient (wet organ weight/bw) X 100 for testes and epididymis of each animal were calculated and tabulated [42].

Blood collection for hormonal assay

Blood was collected immediately after anesthesia. Sera were separated by centrifugation the blood at 4500 rpm for 30 min and kept at -20 °C for subsequent use for biochemical hormonal profile and oxidative stress assay. Testosterone assay was determined using radioimmunoassay (RIA) following the procedure of the kit introduction [43].

Testicular tissue preparation for the biochemical assays

The left testes were rinsed in ice-cold 50 mM sodium phosphate buffer (pH 7.4) containing 0.1 mM ethylene diamine tetra acetic acid (EDTA). The supernatant was separated by means of centrifugation at 1000g for 20 min at 4 °C. The supernatants were used for analyze the antioxidant enzymes.

Superoxide dismutase (SOD)

The specific activity of superoxide dismutase (SOD) was assayed according to **Misra and Fridovich [44]**. Ten microliters of tissue homogenate were added to 970 μ l EDTA–sodium carbonate buffer (0.05 M) at pH 10.2. The reaction was started by adding 20 μ l of epinephrine (30 mM). The assay procedure involves the inhibition of epinephrine auto-oxidation in an alkaline medium (pH 10.2) to adrenochrome, which is markedly inhibited by the presence of SOD.

Lipid peroxidation (LPO) level

The extent of Lipid peroxidation in supernatant of the homogenate testicular tissue was determined by the quantity of malondialdehyde formation (MDA) using the method of **Ohkawa et al. [45]**. Tissue supernatant was mixed with 1 ml TCA (20%) and 2 ml thiobarbituric acid (TBA, 0.67%) and was heated for 1 h at 100 °C. After cooling, the precipitate was removed by centrifugation. The absorbance of the sample was measured at 535 nm.

Epididymal sperm characteristics

Sperm count

To measure sperm reserves, the semen contents of epididymides were minced and diluted in 2 ml of physiological saline solution containing 4% trypan blue [46]. 20 µl aliquots were placed on the Neubauer hemocytometer for counting the number of sperms/mg of epididymis. The total sperm count in squares of 1mm² each was determined to express the number of spermatozoa/epididymis.

Sperm viability

One drop of freshly collected semen (10 µl) was placed on a slide and stained with two drops of freshly prepared staining solution of eosin–nigrosin (1 g eosin + 5 g nigrosin/100 ml deionized water) [47]. The live unstained (intact) and dead spermatozoa (purple to red-stained head) were analyzed under the microscope at X 400.

Sperm motility

Sperm motility was assessed by counting all progressive motile (effective), the non-progressive motile (non-effective or sluggish) and the immotile (dormant) spermatozoa in the same microscopic field (400 X). In each semen sample, at least 10 microscopic fields were examined with at least 100 sperm/field was counted. The percentage of motile spermatozoa was determined by dividing the number of motile sperm cells in each field on the total sperm number X 100 [48].

Sperm morphology

To assess the spermatozoa morphologic abnormalities, a drop of sperm suspension was smeared on a slide, air-dried and stained with 1% eosin Y and 5% nigrosin. The morphological sperm defects were examined under the light microscope using 400X [48]. At least one hundred spermatozoa from different fields in each slide were examined and classified for criteria of morphological abnormalities (head and tail) according to **Filler [49]**. Abnormal sperm shape in head and tail was counted, photographed and the percentage was calculated and tabulated.

Epididymal sperm chromatin (DNA integrity)

Acridine orange staining was used to display the effects of AgNPs on epididymal sperm chromatin (DNA quality and integrity). Smears of epididymal suspensions were fixed in Carnoy's fixative for at least two h. The slides were stained with acridine orange for 5 min and gently rinsed with deionized water. Two-hundred sperms from each staining slide were evaluated as follows: green sperm heads as normal DNA, yellow or orange to red sperm heads as damaged DNA [50].

Histopathological studies

At the end of the experiment, the testicular tissue samples were collected just after sacrifice, fixed in 10 % formalin, dehydrated, embedded in paraffin wax according to the routine processing protocol. Sections of 5 μm slices were stained with hematoxylin and eosin [51], examined and photographed by the light microscopy.

Electron microscopic investigation

Small pieces of testes were fixed in 4% formalin and 1% glutaraldehyde (4F1G) fixative mixture in 0.1 M phosphate buffer (pH 7.4) for 24 h at 4 °C. Then, specimens were post fixed in 2% osmium tetroxide (OsO₄) at the same buffer for 2 h at 4 °C. Tissues were washed in the buffer and dehydrated at 4 °C through a gradual series of ethanol, embedded in Epon-araldite resin mixture. Semithin sections (1 μm) stained with Toluidine blue were examined and photographed using LM. Ultrathin sections (60 nm thick) were double stained with uranyl acetate for 1/2 hr and lead citrate for 20-30 min and examined by Joel TEM [52].

Statistical analysis

For statistical analyses, the SPSS for windows software package version 18.0 (SPSS, Chicago, IL, USA) was used. Data was given in the form of arithmetical mean values and standard deviations. One-way analysis of variance (ANOVA) was performed and variant groups were determined by means of the Duncan test. *p* value was assumed to be significant at 0.05.

RESULTS

Animal observation, body weight and the reproductive organs weight

The overall behavior of animals belonging to the all experimental mice injected i.p. with the different concentrations (100, 500 & 1000 mg/kg) of silver nanoparticles (AgNPs) were similar. During the first few days after treatment, several stress symptoms (poor appetite and increased aggression) were observed in all AgNPs-treated groups. Only one mouse was died at the third week of treatment with 1000 mg/kg AgNPs and the results exerted no significant decreases in body weight changes, coefficient-relative testes or epididymes weights in all treatments, relative to the control (**Table 1**).

Table 1: Mice male indices after i.p. exposure to different concentrations of silver nanoparticles (AgNPs) for 28 days.

Parameters	Silver nanoparticles (AgNPs) (mg/kg)			
	0 mg/kg	100 mg/kg	500 mg/kg	1000 mg/kg
Assigned male mice	10	10	10	10
Lethality	0	0	0	1
Body weights (g)				
Initial	32.7 ± 2.98	31.6±2.11	33.4±2.89	33.5 ± 3.01
Final	48.5 ±4.11	46.7 ± 3.98	48.9±4.11	49.1 ± 3.69
Body weight change %	48.32±4.65	47.78±4.1	46.41±3.98	46.57±4.21
•Organ weight coefficients (mg/g)				
Testes	0.52 ±0.042	0.54 ± 0.061	0.51 ±0.041	0.49 ±0.031
Epididymes	0.09 ± 0.003	0.08 ± 0.002	0.06 ± 0.004	0.04 ± 0.001

All data are measured in mean ±SD

•Organ weight coefficient (mg/g) = wet organ weight (mg) / Body weight (g) x100%

Notice: No statistic significant differences are recorded among all treatments in the different measurements

Effects of AgNPs on the reproductive hormone

In concentration-dependent of AgNPs, there were decreases in testosterone levels in sera of mice administered i.p. for 28 days, comparing to the control. This decrease was significant in animals exposed to 500 & 1000 mg/kg of AgNPs (**Fig. 1**).

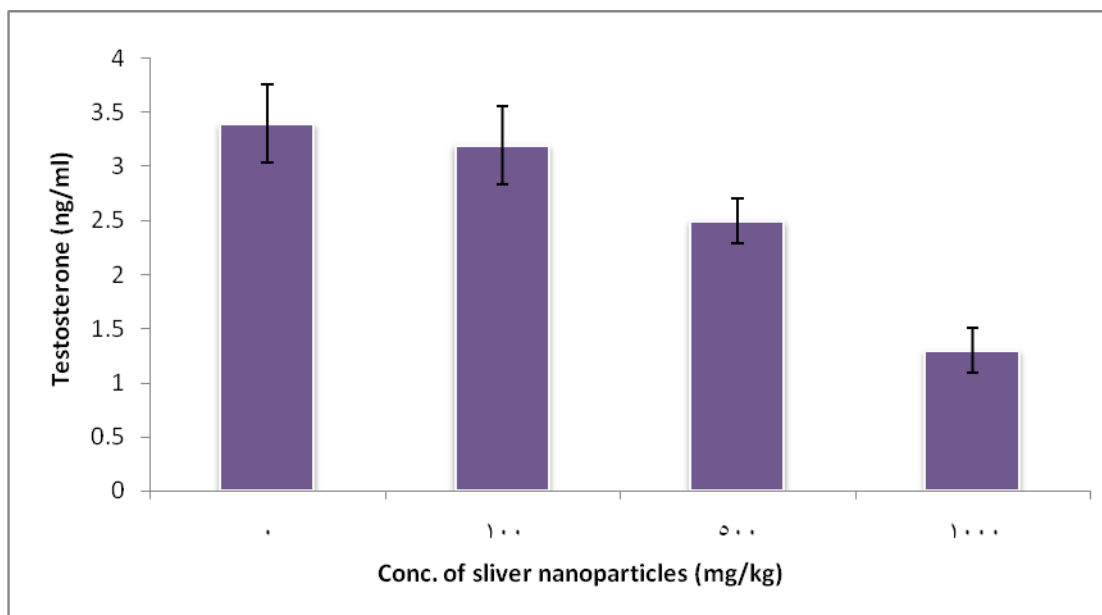


Fig. 1. Serum testosterone levels of male mice administered intraperitoneally with three different concentrations of silver nanoparticles (AgNPs) for 28 days.

Biochemical parameters

Compared to the control mice and 100 mg/kg bw of AgNPs-treated mice, the results revealed significant decrease in superoxide dismutase (**SOD**) activity and significant increase in the level of lipid peroxidase (**LPO**) in the testicular tissue of mice treated with 500 and 1000 mg/kg AgNPs (**Fig. 2 A, B**).

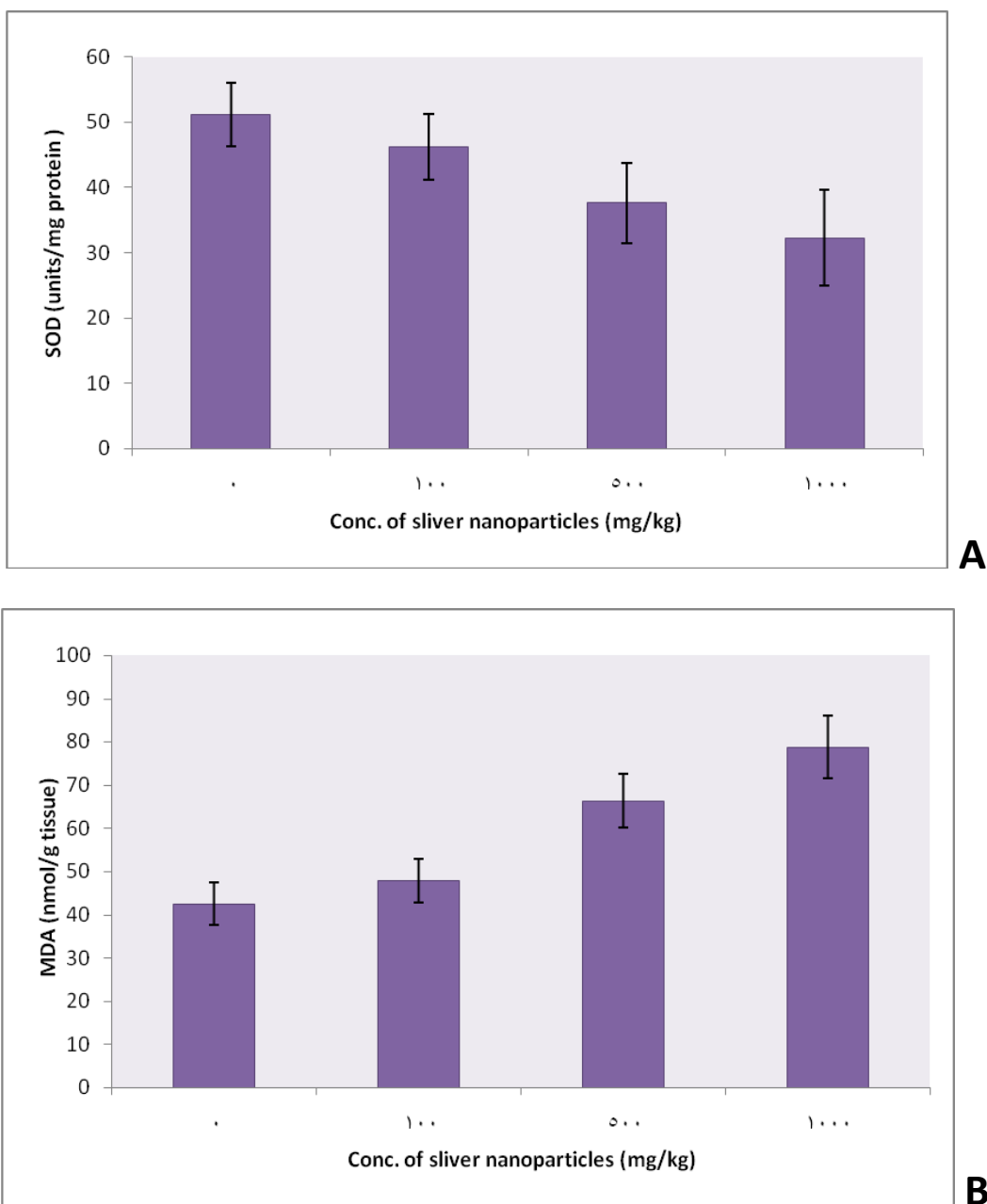


Fig. 2 (A,B). Activities of superoxide dismutase (SOD) and Lipid peroxidation expressed by malonaldehyde (MDA) in the testicular tissues of mice administered intraperitoneally with three different concentrations of silver nanoparticles (AgNPs) mg/kg for 28 days.

Sperm characteristics

The results revealed a concentration dependent significant reduction in sperm production, viability as well as in the non-progressive and immotile sperms in the epididymis of 500 & 1000 mg/kg AgNPs-treated mice, compared with the control. However, there was significant decrease in the progressive sperm motility in the epididymes mice treated with 1000 mg/kg AgNPs (**Table 2**).

Further, there were significant increases in percentage of sperms with abnormal morphology, depending on concentrations of nanosilver particles (**Table 2**), and these increases were prominent in the head region more than the tail. Of such results, most spermatozoa end up with a variety of abnormal morphologies, where the various head abnormalities included amorphous, calyculate, and inverted head. However, the major tail abnormalities were curved, irregular or coiled (**Fig. 3 (1A & 2B-K)**).

Table 2: Sperm characteristics of male mice after i.p. exposure to three different concentrations of silver nanoparticles for 28 days.

Sperm Parameters	Silver nanoparticles (AgNPs) (mg/kg)			
	0	100	500	1000
Count/epididymis ($\times 10^6$)	96.1 \pm 8.98 ^a	94.7 \pm 7.26 ^a	73.7 \pm 6.25 ^b	45.6 \pm 3.11 ^c
Motility (%)				
Progressive	79.9 \pm 6.25 ^a	75.5 \pm 6.07 ^a	76.3 \pm 7.11 ^a	71.1 \pm 6.98 ^b
Non-Progressive	10.4 \pm 0.89 ^a	11.2 \pm 0.97 ^a	12.4 \pm 1.08 ^a	15.5 \pm 1.62 ^b
Immotile	9.7 \pm 0.89 ^a	13.3 \pm 1.21 ^b	11.2 \pm 0.98 ^c	13.4 \pm 1.05 ^b
Morphology (%)				
Normal	94.5 \pm 9.11 ^a	92.4 \pm 8.96 ^a	68.8 \pm 5.98 ^b	34.6 \pm 2.68 ^c
Abnormal head	2.6 \pm 0.23 ^a	4.3 \pm 0.36 ^b	24.9 \pm 0.21 ^c	46.8 \pm 3.98 ^d
Abnormal tail	2.9 \pm 0.29 ^a	3.2 \pm 0.365 ^a	6.3 \pm 0.58 ^b	18.6 \pm 1.36 ^c
Total abnormalities	5.5 \pm 0.56 ^a	7.5 \pm 0.81 ^b	31.2 \pm 2.01 ^c	65.4 \pm 5.98 ^d
Viability (%)	97.8 \pm 9.98 ^a	96.5 \pm 9.79 ^a	83.1 \pm 8.01 ^b	52.3 \pm 2.98 ^c
DNA integrity (acridine orange)	84.3 \pm 7.58 ^a	86.2 \pm 6.98 ^a	76.8 \pm 6.25 ^b	54.5 \pm 4.39 ^c

All data are measured in mean \pm SD

Letters (a,b,c): means that there is significant differences in all treatments, compared to at $p \leq 0.05$.

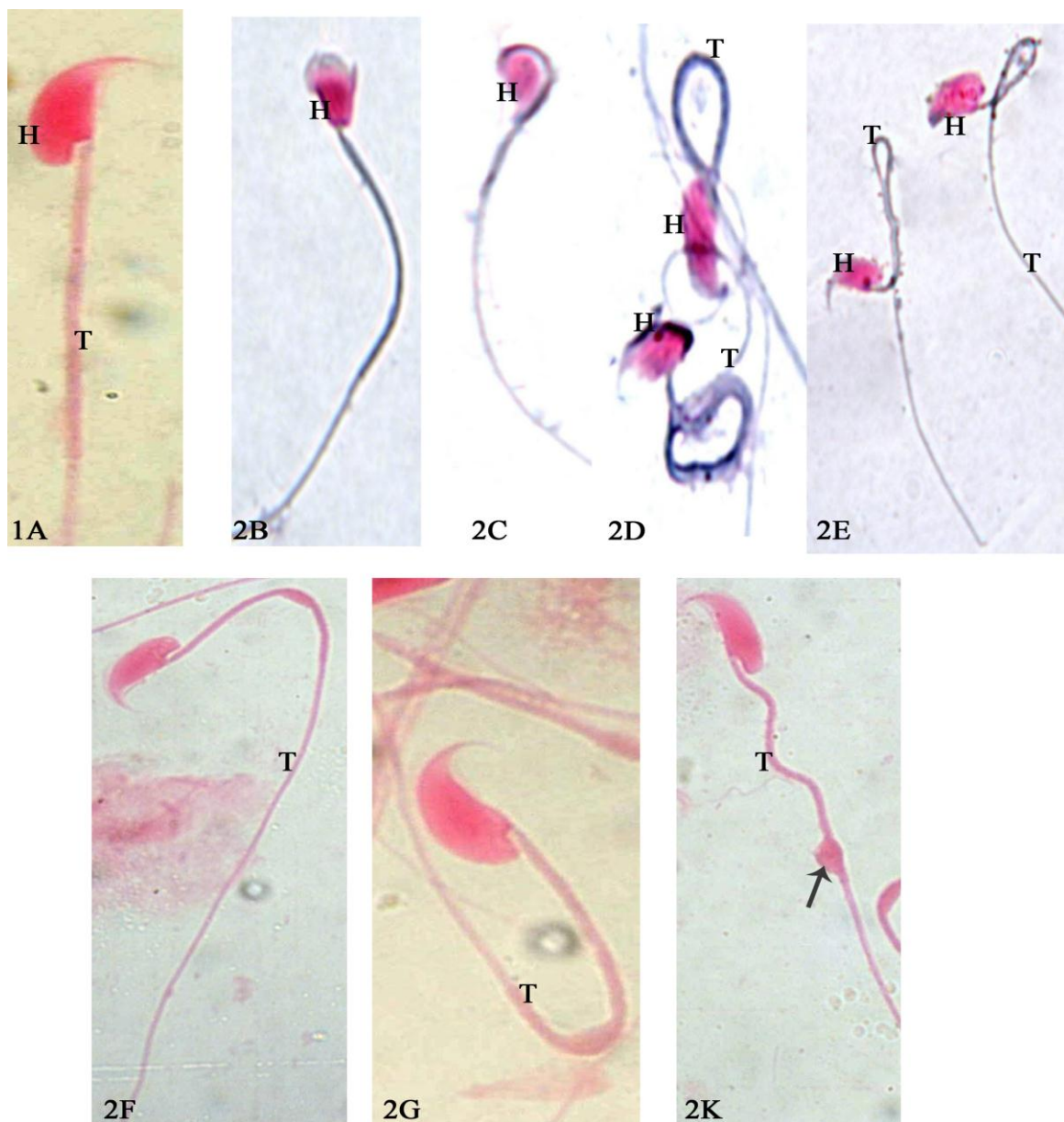


Fig. 3. Showing, 1A: Normal sperm shape in the epididymal semen of mice showing: (H): Head; (T): Tail. (2): Different pattern of abnormalities in epididymal semen of AgNPs-treated mice, showing: B: amorphous head (H); C: calyculate head (H); D & E: inverted heads (H) and curved tails (T); F & G: curved tails (T); (K) irregular tail (T) and cytoplasmic droplet (arrow). X 1000.

DNA sperm chromatin

By using Acridine orange stain, the results revealed that most sperm heads in the epididymes of 500 and 1000 mg/kg AgNPs-treated mice appeared red in color, indicating to the significant decrease in DNA sperm quality, However, in the control mice as well as in 100 mg/kg AgNPs-treated mice, the color was green (**Table 2**).

Histological observations of testes of control mice

Hematoxylin and eosin-stained sections of control mice showed mostly normal testicular architecture with an orderly arrangement of germinal cells (spermatogonia, spermatocytes, and different stages of spermatids in addition to spermatozoa) and Sertoli cells. These tissues are separated from one another by a delicate connective tissue stroma (interstitial tissue) containing interstitial Leydig cells that secrete the testicular hormones (**Figs. 4 & 5**).

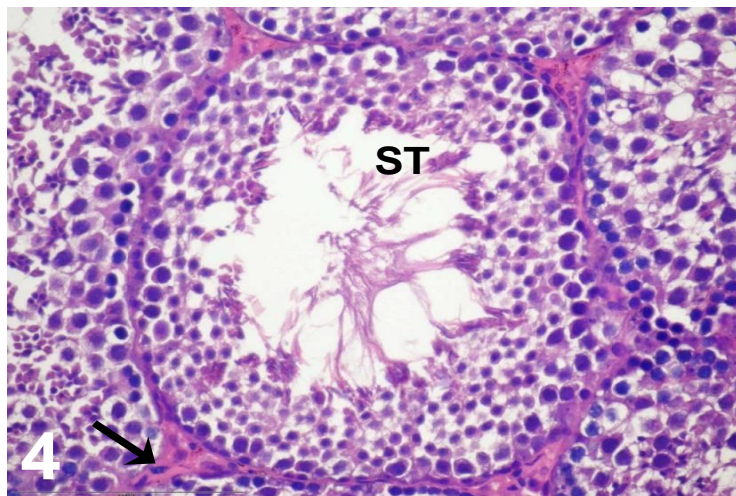


Fig. 4: Light micrograph of section of control testis showing, the appearance of seminiferous tubules (ST) revealing the normal testicular architecture and intact interstitial tissue (arrows). H& E, X 400.

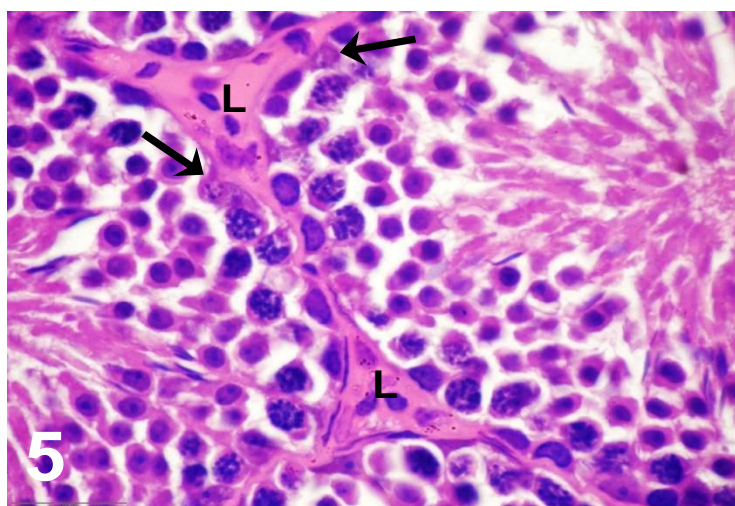


Fig. 5: Enlarged part of the previous figure showing, an orderly arrangement of germinal cells and Sertoli cells (arrows); interstitial tissue contains interstitial Leydig cells (L). H& E, X 630.

Sections of testes of mice administered with 100 mg/kg AgNPs, showed nearly normal histological architecture as shown in the control sections. The spermatogenic layers in seminiferous tubules were arranged normally, and contain the different stages of

spermatogenic epithelium, in addition to the presence of interstitial Leydig cells in the interstitium (Figs. 6, 7).

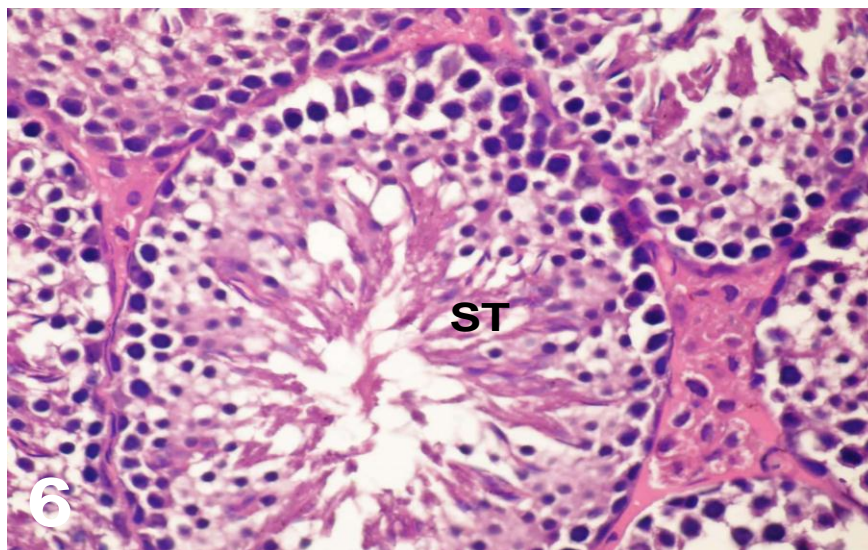


Fig. 6: Light micrograph of section of testis mice administered with 100 mg/kg AgNPs, showing the normal arrangement of spermatogenic cells and Sertoli cells in ST. H& E, X 400.

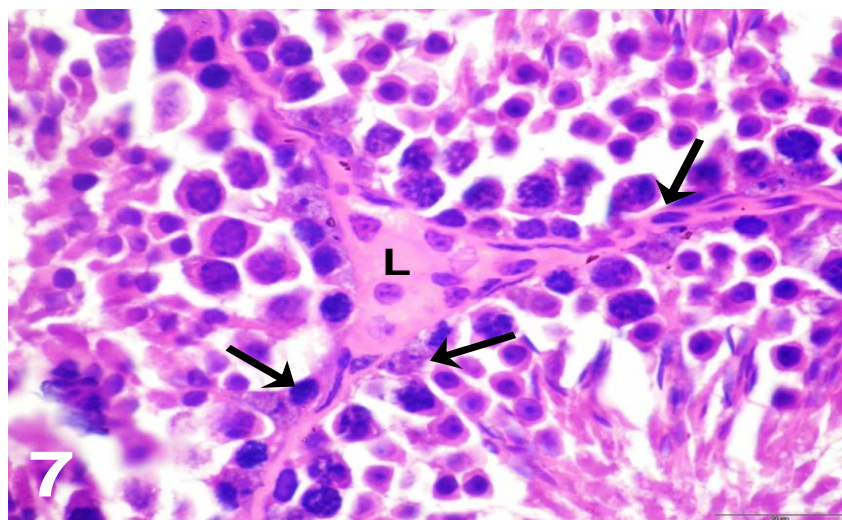


Fig. 7: Enlarged part of the previous figure showing, the different spermatogenic cells; Sertoli cells (S); and the interstitial Leydig cells (L). H& E, X 630.

However, sections in testes of mice administered with 500 and 1000 mg/kg AgNPs revealed disturbed spermatogenic layers. Moderate histopathological changes were seen, such as vacuolation, detachment, and intercellular dissociation of spermatogenic cell lines that caused sloughing of germ cells into the tubular lumen. The degenerative tubules were lined by very few spermatogenic cells. In addition there was marked decrease in spermatozoa in the lumen of seminiferous tubules (Figs. 8 - 11).

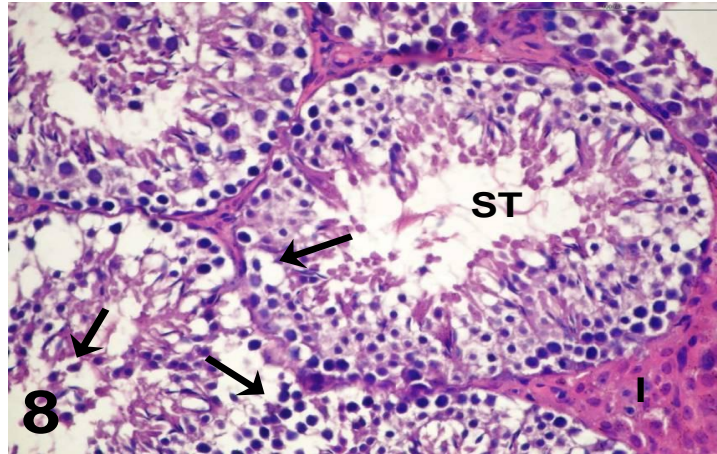


Fig. 8: Light micrograph of section of testis mice administered with 500 mg/kg AgNPs, showing, moderate degenerative changes in ST such as vacuolation (arrows) of the spermatogenic cell lines; Notice: the intact interstitial tissue (I). H& E, X 400.

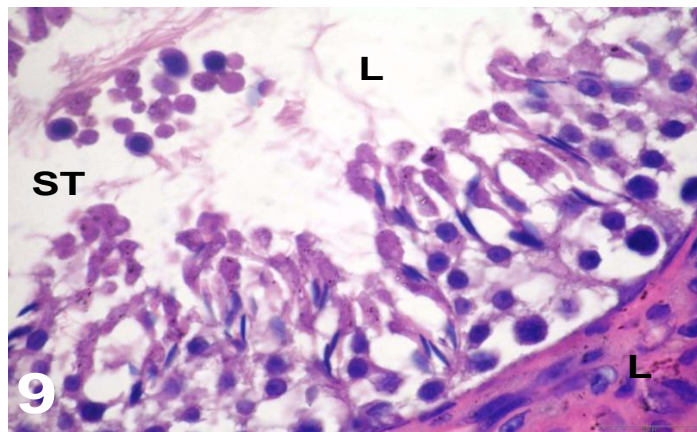


Fig. 9: Enlarged part of the previous figure showing, vacuolation and detachment of the spermatogenic cell lines; Note the marked decrease in the formation of spermatozoa in the lumen of seminiferous tubules (ST) and intact Leydig cells (L) in the interstitial tissue. H& E, X 1000.

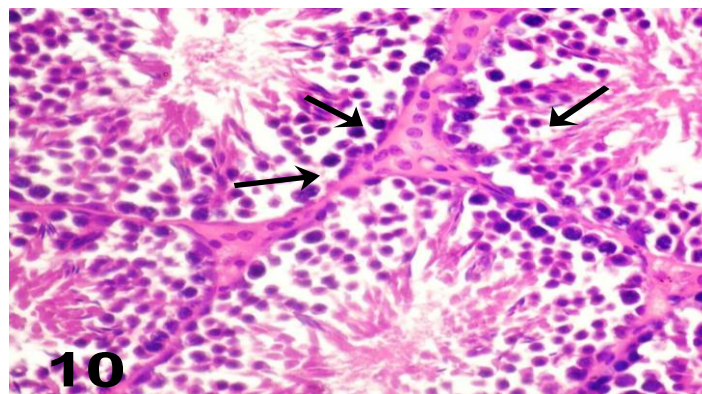


Fig. 10: Light micrograph of section of testis mice administered with 1000 mg/kg AgNPs,, showing the degenerative changes (arrows) in many seminiferous tubules; Note the marked loss in spermatozoa in the lumen of these tubules . H& E, X 200.

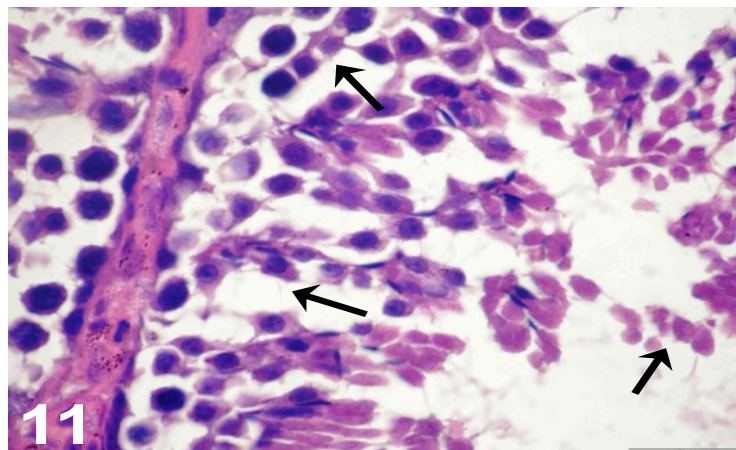


Fig. 11: Enlarged part of the previous figure showing, detachment, sloughing and loss in spermatogenic cells (arrows); Note that the absence of mature spermatozoa in the lumen of ST. H&E, X 1000.

Semithin sections of control testes revealed the orderly arrangement germinal cells in most seminiferous tubules (**Fig. 12**), and the presence of normal stages of zygotene spermatocytes, secondary spermatocytes and different steps of spermatids. Such spermatids appeared projecting into the lumen but still adherent to the Sertoli cells (**Fig. 13**). **Figure 14** reveals the nearly normal testicular architecture of mice treated with 100 mg/kg AgNPs, where most spermatogenic stages are observed, and the mature spermatozoa are projected towards the Sertoli cells.

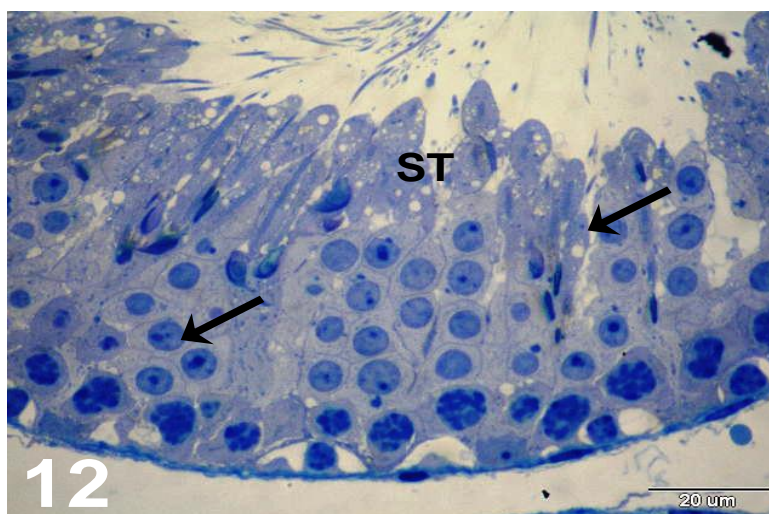


Fig. 12: Light micrograph of a semithin section of control testis, showing the normal testicular architecture with an orderly arrangement of germinal cells (arrows). Toluidine blue stain, X 200.

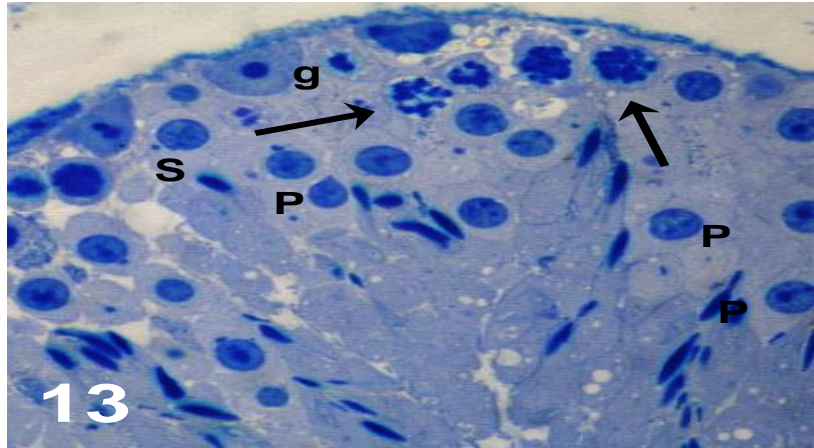


Fig. 13: Light micrograph of a semithin section of control testis, showing the presence of normal stages of zygotene spermatocytes (arrows), spermatogonia (g); different steps of spermatids (P)(rounded and elongated); Note that such spermatids are projecting into the lumen of ST and still adherent to the Sertoli cells (S). Toludine blue stain, X 200.

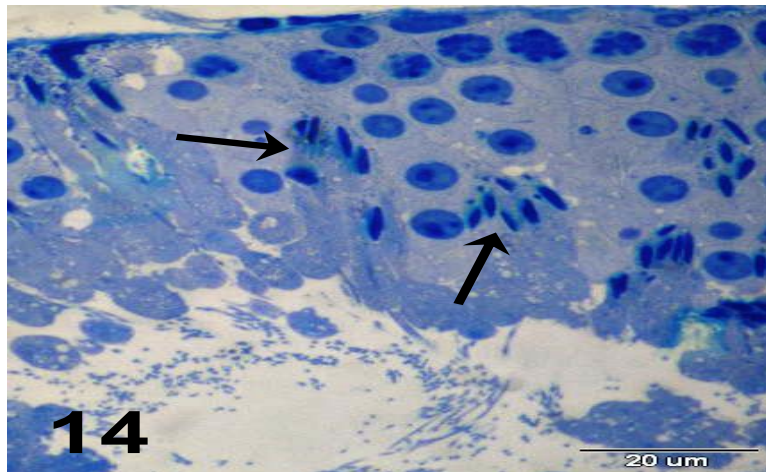


Fig. 14: Light micrograph of a semithin section of testis mice administered with 100 mg/kg AgNPs, showing the normal testicular architecture with an orderly arrangement of germinal cells; Note that the mature spermatozoa (arrows) are projected to the Sertoli cells. Toludine blue stain, X 200.

Further, administration with high doses AgNPs (500 & 1000 mg/kg), revealed some disruption in the testicular architecture and there was marked loss in spermatogenic stages, testicular atrophy and loss in height of spermatogenic epithelium (**Figs. 15-17**). This indicates the decrease in the different stages of spermatids and mature spermatozoa.

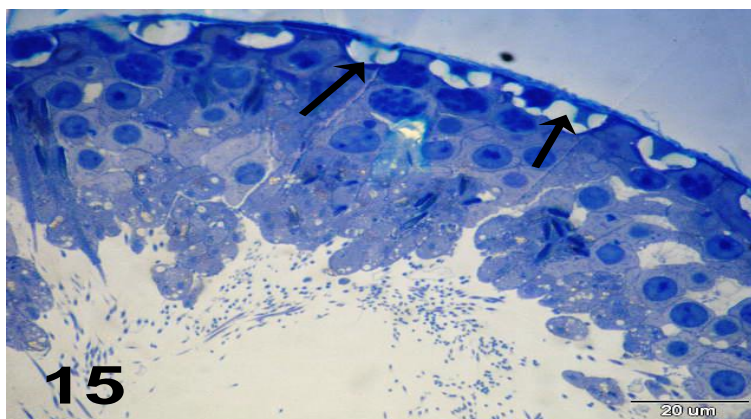


Fig. 15: Light micrograph of a semithin section of testis mice administered with 500 mg/kg AgNPs, showing disruption and degeneration of spermatogonia (arrows) the testicular architecture with marked loss in spermatogenic layers. Toluidine blue stain, X 200

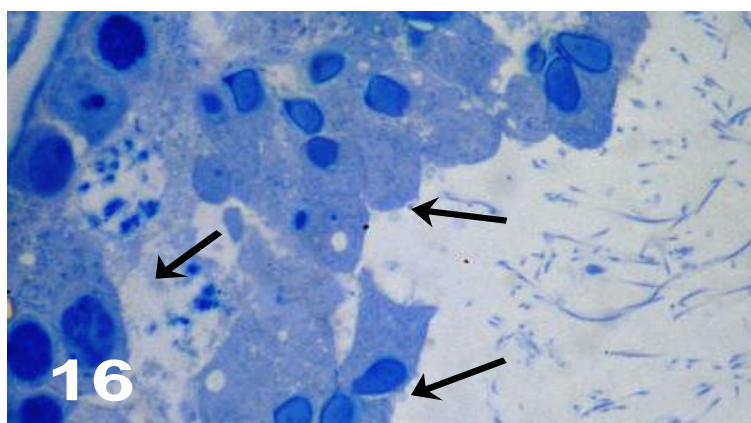


Fig. 16: Light micrograph of a semithin section of testis mice administered with 1000 mg/kg AgNPs, showing severe degeneration in most spermatogenic stages (arrows) and marked loss in spermatogenic stages. Toluidine blue stain, X 400.

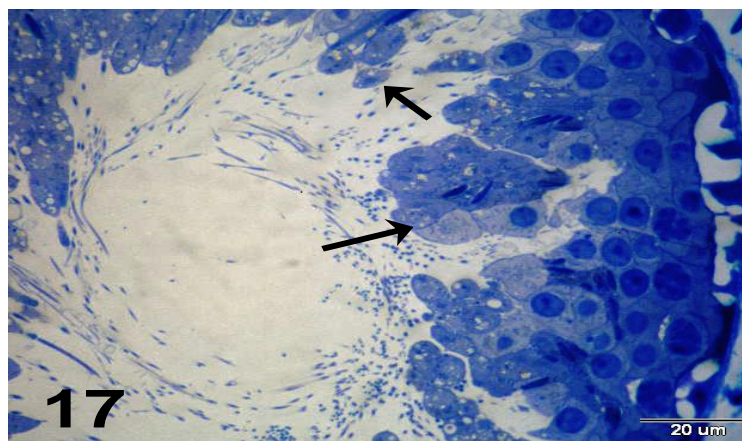


Fig. 17: Light micrograph of a semithin section of testis mice administered with 1000 mg/kg AgNPs, showing testicular atrophy and loss in height of spermatogenic epithelium. Toluidine blue stain, X 400.

The electron micrographs of testis of control mouse showed the presence of tightly and orderly arranged spermatogenic stages, namely the spermatogonia, spermatocytes, spermatids, and finally mature spermatozoa (Figs. 18, 19). Spermatogonia are the stem cells of the germ cell population that divide mitotically to produce the primary spermatocytes. These cells appeared close to the basement membrane of the tubules, and their nuclei appeared small and dark. The primary spermatocytes are large cells, having large spherical nuclei which are characterized by the presence of chromosomes in various dividing stages (Fig. 18).

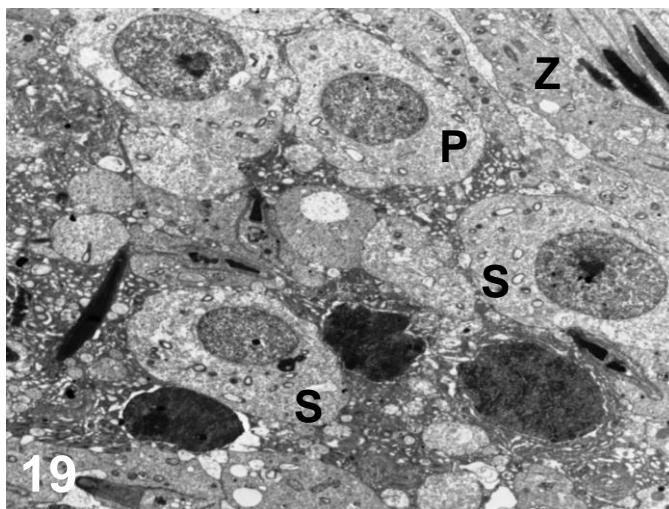


Fig. 18: Electron micrograph in testis of control mice, showing the tightly and orderly arrangement of different spermatogenic stages, namely spermatocytes (S), spermatids (P) and spermatozoa (Z). X2000.

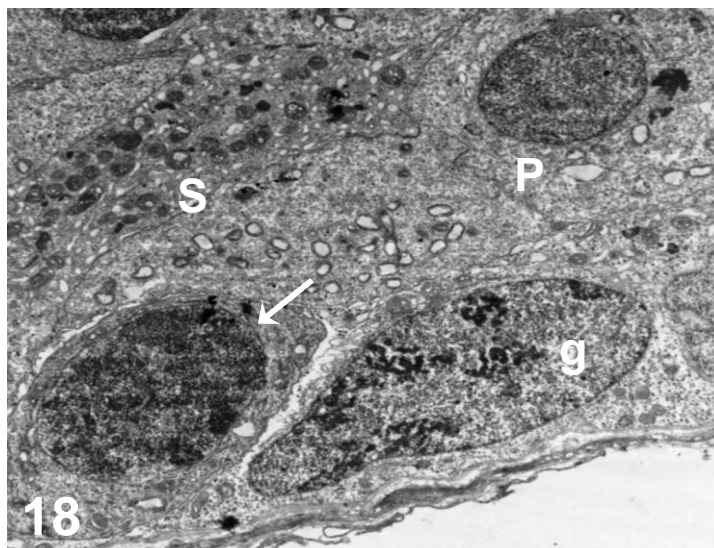


Fig. 19: Electron micrograph in testis of control mice, showing different spermatogenic stages, namely the spermatogonia, primary spermatocytes (arrow), spermatids (P) and part of cytoplasm of Sertoli cell (S). X 2000.

The secondary spermatocytes exhibited a pale stained homogeneous chromatin, and centrally located large clumps of chromatin material (**Fig. 19**). These cells are rarely observed, where they are resulting from the first meiotic division of the primary spermatocyte. Their life span is short and enters into the second meiotic division producing the spermatids. Also, they exhibited a pale stained homogeneous chromatin, and often exhibited centrally located large clumps of chromatin material.

Two types of spermatids are recognized (early and late). The early stages of developing acrosomal cap are small in size and rounded in shape, having large spherical nuclei with an area of condensed chromatin. The late stages showed different degrees of nuclear elongation and variable positions in relation to the surface of the supporting Sertoli cells (**Fig. 19**). Each Sertoli cell rests on/and adheres to the basal lamina, filling the narrow space between the cells of the spermatogenic series and their apical ends frequently extended into the lumen of the seminiferous tubules (**Fig. 19**).

Marked ultrastructural changes are observed in the testicular tissue of mice treated with 100 mg/kg AgNPs, except small intercellular spaces were observed among spermatogenic stages (**Fig. 20**). The primary spermatocytes, secondary spermatocytes and spermatozoa are clearly observed in many sections (**Fig. 21**).

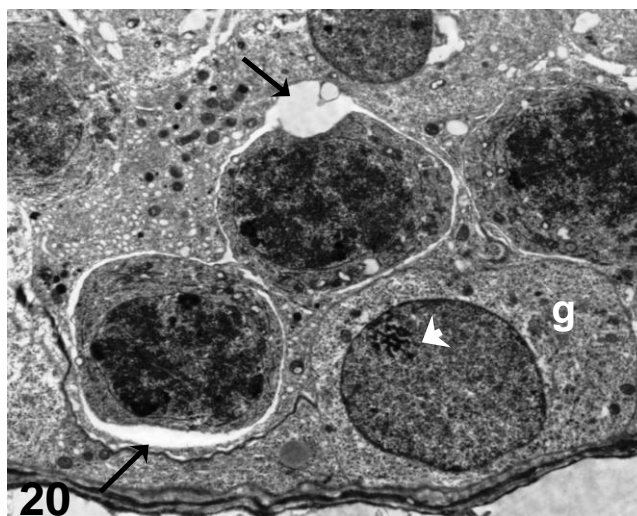


Fig. 20: Electron micrograph in testis mice administered with 100 mg/kg AgNPs, showing, the presence of intercellular spaces (arrows) between the spermatogenic cells; spermatogonia (g) having small condensed chromatin (arrowhead). X 3000.

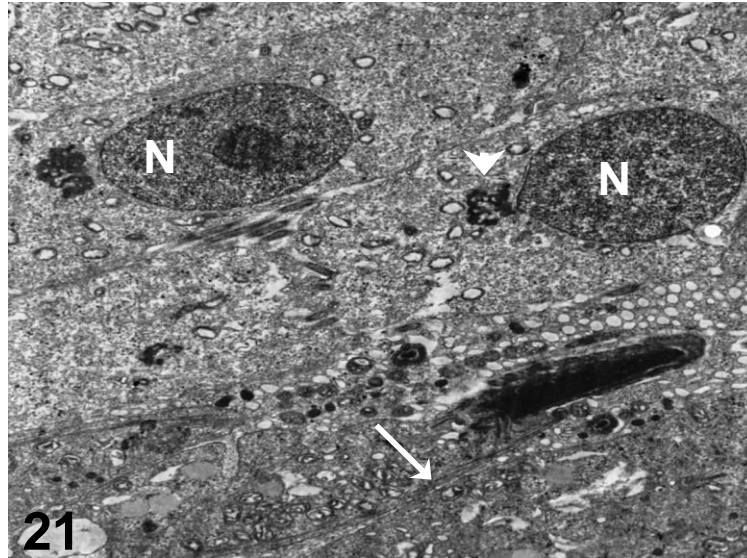


Fig. 21: Electron micrograph in testis mice administered with 100 mg/kg AgNPs, showing the nuclear elongation of spermatids (N); Note the formation of the microtubular manchette (arrow) and the presence of chromatoid body (arrowhead) near the base of the nuclei. X2000.

Ultrastructural appearance of testes of mice administered with 500 mg/kg showed the presence of intercellular spaces between the spermatogenic cells (**Fig. 22**). Most spermatogenic stages appeared normal, and the spermatozoa are extending to the Sertoli cells. However, marked vacuolation in the cytoplasm of most spermatids was observed; in addition to the appearance of many stages of secondary spermatocytes (**Figs. 23, 24**).

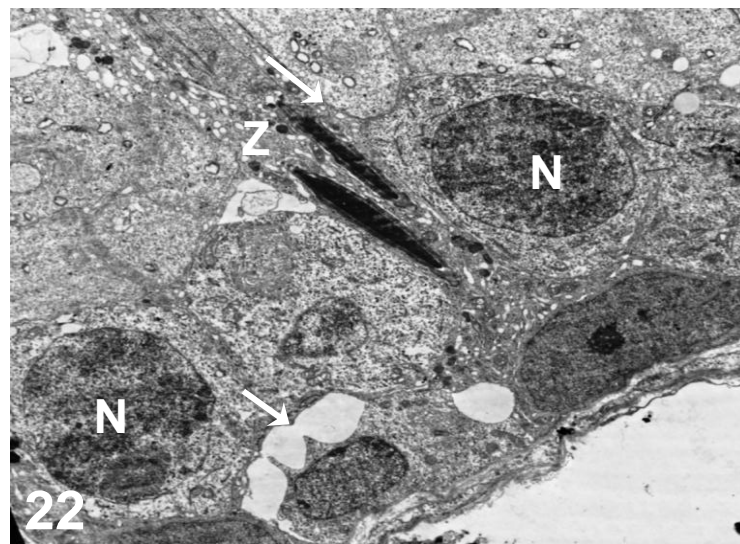


Fig. 22: Electron micrograph in testis mice administered with 500 mg/kg AgNPs, showing wide intercellular space (arrow) among spermatogenic stages; nuclei (N) of primary spermatocytes; Note the already organized spermatozoa (Z) having mitochondrial sheath (in the midpiece) and the fibrous sheath (in the principal piece). X2000.

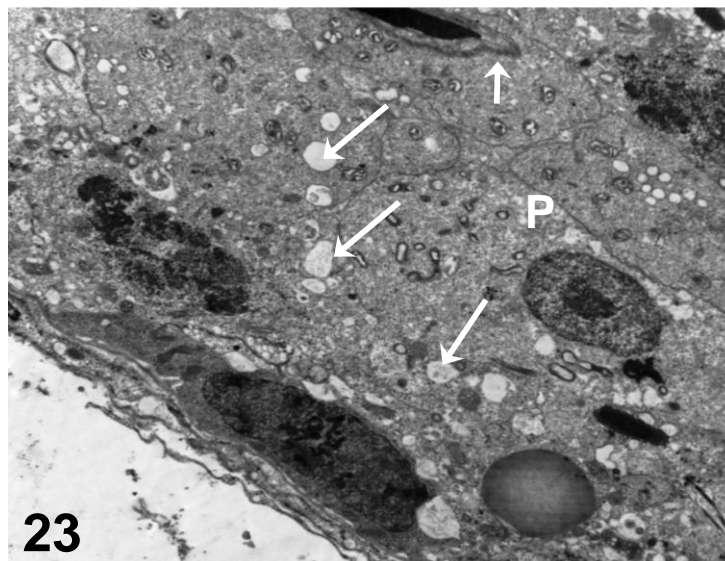


Fig. 23: Electron micrograph in testis mice administered with 500 mg/kg AgNPs, showing the appearance of vacuolation (arrows) in the cytoplasm of spermatids (P); Note the appearance of abnormal formation of acrosomal sheath (arrowhead) in spermatozoa. X 2000.

Further, the more developed spermatids exhibited some structural alterations and considerable degrees of deformation in the formation of the acrosomal sheath, where the acrosomal vesicle was found inside the nucleus instead of being on it (**Fig. 24**).

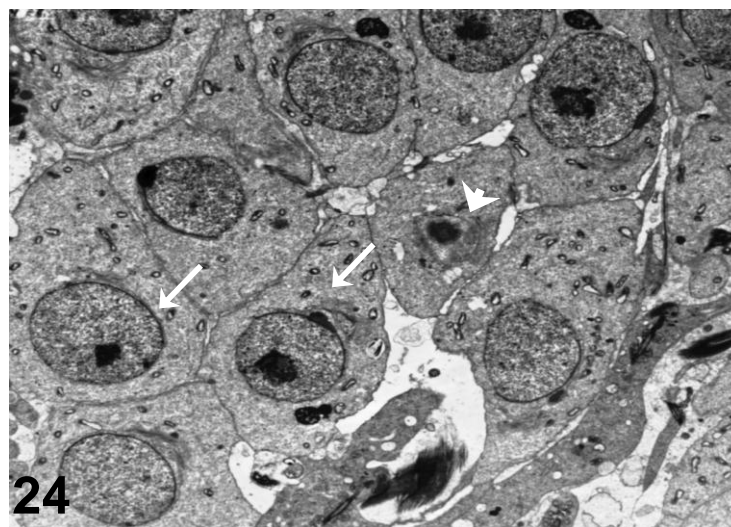


Fig. 24: Electron micrograph in testis mice administered with 500 mg/kg AgNPs, showing the appearance of many stages of secondary spermatocytes (arrows); Note: the acrosomal vesicle (arrowhead) found inside the nucleus instead of on it (arrowhead). X 2000.

In sections of testes of mice treated with 1000 mg/kg AgNPs, there was marked disruption in the arrangement of spermatogenic layers. The ultrastructural alterations recorded

coincide with the histological findings, where the dissociation of germ cells are in parallel with the appearance of wide intercellular spaces (Fig. 25). The spermatogenic cells, especially the primary spermatocytes showed degenerative changes where they contained abnormally condensed nuclei (Fig. 26).

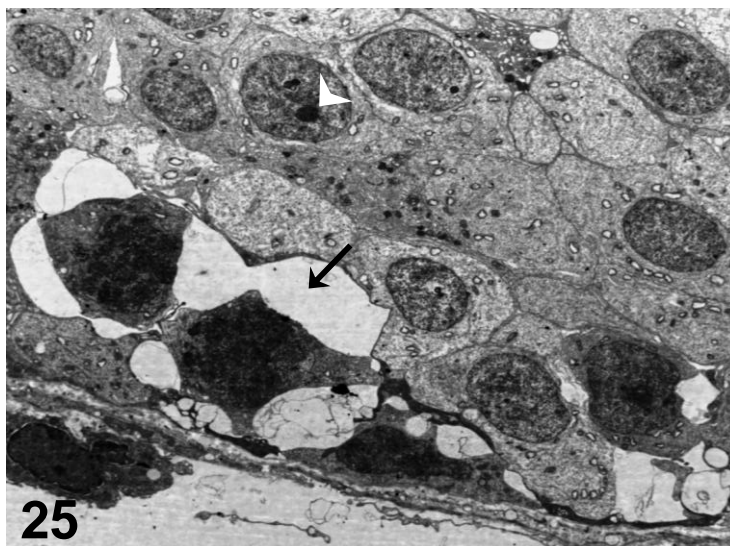


Fig. 25: Electron micrograph in testis mice administered with 1000 mg/kg AgNPs, showing the appearance of wide intercellular spaces (arrow) among the the dissociated spermatogenic stages; Note the appearance of acrosomal vesicle (arrowhead) found inside the nucleus instead of on it. X 2000.

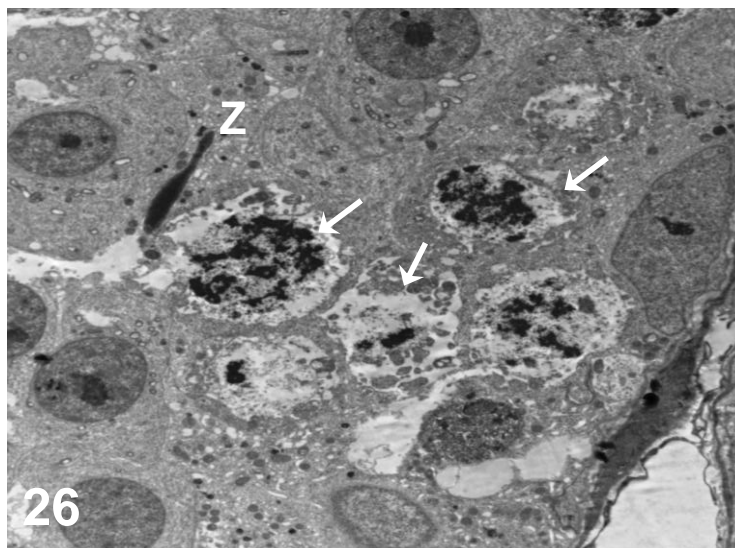


Fig. 26: Electron micrograph in testis mice administered with 1000 mg/kg AgNPs, showing the abnormal condensation of chromatin in the nuclei of spermatocytes (arrows); Note: the appearance of abnormal-shaped spermatozoa (Z). X 3000.

Also, the spermatids exhibited severe alterations, and numerous large vacuoles appeared inside the cytoplasm. In addition, there was variety of abnormal-shaped late

spermatids and spermatozoa, such as with irregularly shaped acrosome and/or nuclei. In late stages of spermatids, the acrosome stretched (elongated) unusually (**Figs. 27, 28**).

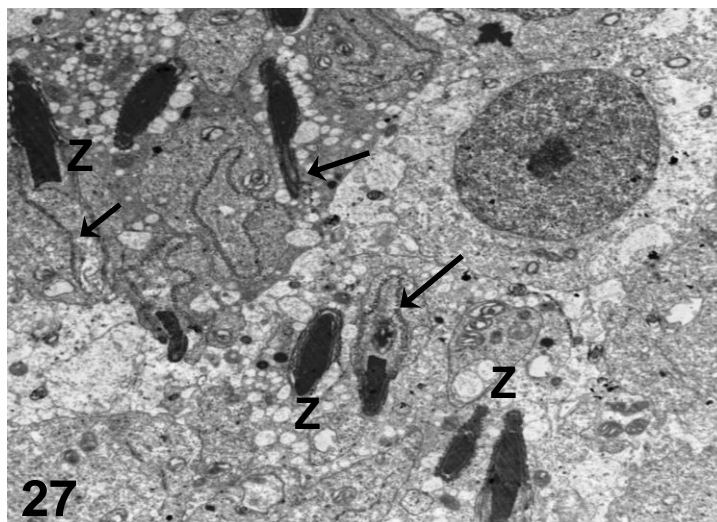


Fig. 27: Electron micrograph in testis mice administered with 1000 mg/kg AgNPs, showing a variety of the nuclear shape in the formation of spermatozoa (Z); arrows point at acrosome are stretched unusually. X 3000.

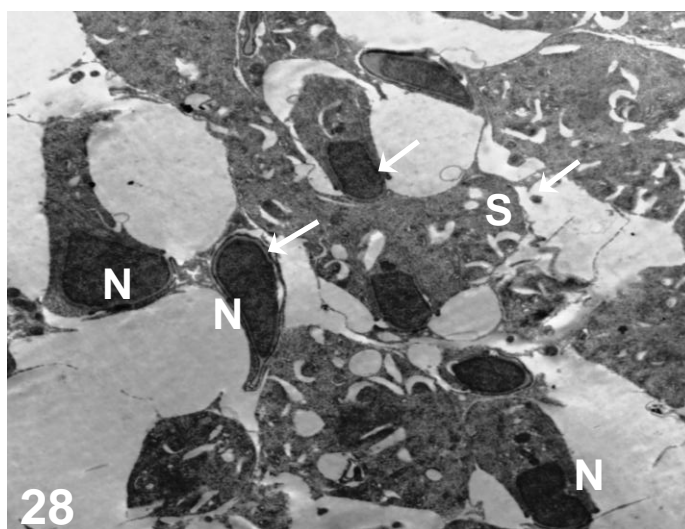


Fig. 28: Electron micrograph in testis mice administered with 1000 mg/kg AgNPs, showing the appearance of spermatozoa in cross section of the highly vacuolized Sertoli cell (S); Note the small, blunt or deformed-shaped nuclei (N) of the developing spermatozoa (arrows). X 3000.

Furthermore, in the interstitial tissue, some Leydig cells contained are apparently irregular and deformed in shape and the chromatin was found as thin patches in the electron lucent nucleoplasm. The cytoplasm of these cells contained many vacuoles (**Fig. 29**).

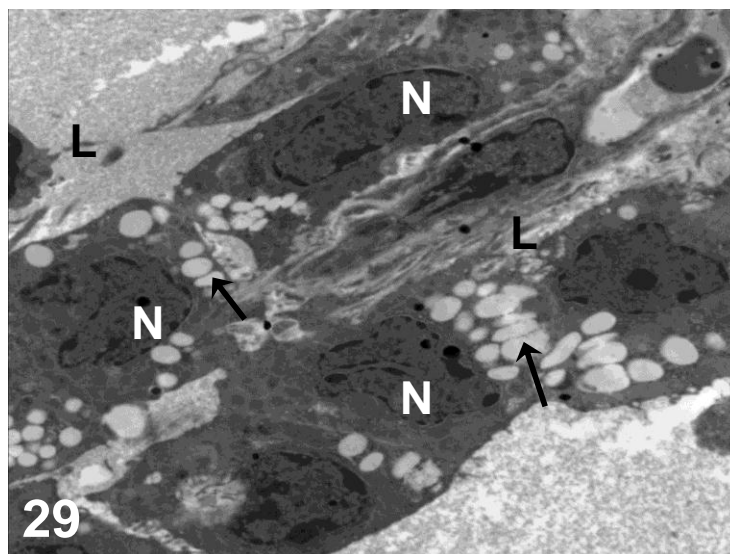


Fig. 29: Electron micrograph in testis mice administered with 1000 mg/kg AgNPs, showing, thenuclei (N) of Leydig cells (L) in the interstitial tissueare apparently irregular and deformed in shape and the chromatin was found as thin patches in the electron lucent nucleoplasm; Note that the cytoplasm contains many vacuoles (arrows). X 2500.

DISCUSSION

The reproductive and developmental toxicity of nanomaterials has become increasingly recognized as an important part of the nanotoxicology [38]. In the current study we evaluated the possible damaging effect of silver nanoparticles (AgNPs) on the reproductive performance and the testicular tissue of mice was examined.

Daily intraperitoneal administration of AgNPs for 28 days at concentrations of 100, 500 and 1000 mg/kg showed no statistically significant differences in body weight as well as testes and epididymis weights, compared to the control animals. **Gromadzka-Ostrowskaa et al. [31]** revealed that intravenous exposure of rats to AgNPs caused no change in body weight and organs weight between experimental groups and control animals. **Garcia et al.[10]** found that low dose (1 mg/kg/dose) AgNPs that intravenously injected into male CD1 mice over 12 days, resulted in no changes in body and testis weights as well as sperm concentration. However, **Shahare and Yashpal [53]** observed that oral exposure in mice for 21 days.

Most striking finding in this study is the reduction in the number of sperm count, viability, forward progressive sperm motility in the epididymis of AgNPs-treated mice, depending on concentration. However, dead sperms, and DNA sperm damaged were increased markedly. Sperm count is considered to be one of the important factors that affect fertility [54]. **Gromadzka-Ostrowskaa et al. [31]** found that a size-dependent (20 nm and 200 nm), dose-dependent (5 and 10 mg/kg body mass) and time-dependent (24 h, 7 and 28 days) decrease the epididymal sperm count in rats, and an increase in number of dead sperms after treatment with AgNPs. These results are in consistence with the suggestion of **Kruszewski et al. [55]** who reported that AgNPs could react with cellular DNA and stimulated inflammation, oxidative

damage and cellular dysfunction that created genetic mutation and sperm cells with abnormal morphology. Moreover, **Aitken and De Iuliis [56]** reported that damage to the sperm DNA increases the risk of infertility, miscarriage, or serious disease in the offspring. **Pothuraju and Kaul [57]** postulated that *in vitro* evaluating of buffalo sperm parameters, a dose-dependent decrease in sperm viability and no change in sperm motility.

Moreover, in the present results, spermatozoa end up with variety of abnormal morphologies in both heads and tails, and this increase in abnormalities has reached to maximum at concentration 1000 mg/kg AgNPs. These results are in consisting with the suggestion of **Mangelsdorf *et al.* [58]** who reported that the decrease in the total sperm count, increase in abnormal sperm shape, impair in stability of sperm chromatin or damaged in sperm DNA results in the disruption of spermatogenesis at any stage of cell differentiation.

Furthermore, the biochemical mechanisms in the current findings indicated that injection with high concentrations (500 & 1000 mg/kg) of silver nanoparticles could heighten the level of lipid peroxidation and reduced the activity of antioxidant status as manifested in the primary antioxidant enzyme (superoxide dismutase (SOD)) (indicative of oxidative stress). SOD is the primary step of the defense mechanism in the antioxidant system against oxidative stress by catalyzing the dismutation of 2 superoxide radicals (O_2^-) into molecular oxygen (O_2) and hydrogen peroxide (H_2O_2) [59]. The decrease in SOD suggests an increased superoxide radical production and other ROS induce oxidative damage.

Induction of the oxidative stress is one of the most commonly proposed mechanisms of NPs toxicity [60]. **Asharani *et al.* [27]** suggested that AgNPs can induce disruption of the mitochondrial respiratory chain, therefore increased ROS production and interruption of ATP synthesis, and finally leading to DNA damage. **El-Tohamy [61]** reported that overproduction of ROS can be detrimental to sperm as it is may be associated with male infertility. This could be coincides with the current finding where there was an elevation in the level of lipid peroxidation in the testicular tissue of mice administered with high concentration of AgNPs. The cellular lipid peroxidation indicates that AgNPs induced oxyradicals in the testes tissues. Spermatozoa are susceptible to peroxidative damage because of the high concentration of polyunsaturated fatty acids and a low level of antioxidants [34]. This was consistent with the current results where there was marked reduction in the number of spermatozoa that reflects the fact that AgNPs can impair both sperm cell viability and acrosome reaction.

Plasma testosterone is released from Leydig cells under LH stimulation from the pituitary gland, and it is the principal male sex hormone. Its levels are highest during fetal development during the first few neonatal months; at puberty, when it is required for the development of male secondary sexual characteristics; and throughout the next three to four decades. Also, testosterone is the major androgen, necessary for fetal male sexual differentiation, pubertal development, and the maintenance of spermatogenesis and inhibition of germ cell apoptosis [62][63]. Moreover, testosterone helps in the maturation of round elongated spermatids by promoting the conversion of round spermatid between stages VII and

VIII of the spermatogenic cycle [62]. Also, it acts at the Sertoli cells to regulate spermatogenesis and at the seminiferous tubules to regulate semen production.

Depending on AgNPs concentrations, the present finding showed significant decrease in the level of serum testosterone, and this decrease has strengthened the phenomenon of generation of oxidative stress in the testicular tissue. This could be caused by adverse effects of nanoparticles in the Leydig cells. The reproductive activity in male mammals is dependent on hormonal factors [64]. O'Donnell *et al.* [65] explained that the decrease in testosterone seems to disrupt several mechanisms of germ cell development, and may be the possible cause behind the spermatogenic impairment.

Garcia *et al.* [10] found that sub-acute (short-term) intravenous administration of AgNPs in male mice could be toxic to male reproduction and altered Leydig cell function and testosterone levels.

In the current study, the histological examination and semithin sections of the testis sections taken from 500 & 1000 mg/kg AgNPs-treated mice revealed the loss of the normal cytoarchitecture of seminiferous tubules, detachment and sloughing of seminiferous cellular component, loss in height of spermatogenic epithelium indicating the decrease in the different stages of spermatids and mature spermatozoa.

The nanosilver particles can enter the cell through diffusion or endocytosis to cause mitochondrial dysfunction, generation of reactive oxygen species (ROS), leading to damage to proteins and nucleic acids inside the cell, and finally inhibition cell proliferation. Takeda *et al.* [66] explained that the damaged seminiferous tubules in high dose treated AgNPs may be related to the inhibitory role of the particles in cell proliferation, the effect of nanoparticles on cell cycles and significant decrease of sperm precursor cells or release of them to the mid duct of seminiferous tubules. Many investigators [67][68] suggested that sloughing is caused by the effects of the chemical on microtubules and intermediate filaments of the Sertoli cells, and these effects spread to dividing germ cells and naturally lead to tubular atrophy. The marked decrease in the number of germinal epithelial cells might cause a decrease in the number of spermatocytes and spermatids, which would eventually result in a decrease of spermatozoa. This indicates incomplete spermatogenesis and degeneration of germ cells.

The studies of Hofmann *et al.* [69] and Braydich-Stolle *et al.* [21] showed that AgNPs interfere with spermatogonial stem cell proliferation in a dose-dependent and particle size-dependent manner. They added that, small AgNPs (10–25 nm in diameter) are more likely than larger sized AgNPs (80–130 nm in diameter) to promote apoptosis or the production of reactive oxygen species in these cells. This result is in line with the results of Liu *et al.* [70], suggesting that the small-sized NPs enter the epididymal sperm cells more easily than the larger ones.

Braydich-Stolet *et al.* [21] showed that nanoparticles such as silver and aluminium nanoparticles were able to cross sperm membrane and connect to mitochondria and acrosome

of sperm cells. Also, **McAuliffe et al. [71]** reported that nanoparticles can pass through cell membrane easily and even pass through blood-brain barrier and blood testes barrier.

In the current results, the degenerative histological changes were coincided with the ultrastructural alterations in testes of mice under the effect of different concentrations of AgNPs. One of the most important ultrastructural changes in the testicular tissue of AgNPs-treated mice was the increase in the intercellular spaces between spermatogenic cells. This means dissociation of the Sertoli cells. At any differentiation step (stage), there are complex cellular interactions between the germ cells and the Sertoli cells [72]. In addition, disruption in the spermatogenic cells especially the primary spermatocytes and appearance of much more secondary spermatocytes were observed in many sections. This explains the damaging effect of AgNPs on creating more spermatozoa.

Furthermore, the more developed spermatids exhibited severe structural alterations and variable and considerable degree of deformation in the acrosomal sheath, and the appearance of numerous large vacuoles inside the cytoplasm of most spermatids. These changes may be the results of DNA damage in sperm cells, and the increased frequency of abnormal sperm shape. These data suggest that AgNPs could impair spermatogonial stem cells, since treatment resulted in significant decreases in testis weight and sperm concentrations.

Spermatids are the products of the final meiotic division and found near the lumen of the seminiferous tubules, and they have small spherical nuclei. The more developed spermatids, having the early stages of developing acrosomal cap, and the acrosomal vesicles spread to cover the anterior half of the condensing nucleus and are then known as the acrosome. Also, they undergo an elaborate process of maturation, spermiogenesis to become spermatozoa. Spermatozoa are highly specialized motile cells, each with a single large flagellum formed by maturation (i.e., without further cell division), and it is emerged at the lower region below the nucleus, and a cylindrical bundle of microtubules limits the nucleus laterally. These spermatozoa have very small, highly condensed, oval to conical nuclei. **Miresmaeili et al. [73]** found acute and significant effects of AgNPs on spermatogenesis and on acrosome reaction in sperm cells.

In conclusion, the present study showed that i. p. injection of AgNPs could deteriorate reproductive function of male mice by reduction in sperm production and increased sperm abnormalities. High doses of AgNPs had a negative effect on spermatogenesis process and can influence reproductive potential in mice, while it could not affect fertility of male mice. Also, it was indicated that exposure to AgNPs caused decrease in testosterone and elevation in oxidative status of the testicular tissues as indicated by the reduction in the activity of SOD and the increase in levels of LPO. These results indicated that the effect of AgNPs may be attributed to its oxidative stress.

REFERENCES

- [1] Roduner, E. (2006). Size matters: why nanomaterials are different. *Chem. Soc. Rev.*, 35: 583 – 592.
- [2] Roy, R., Kumar, S., Tripathi, A., Das, M., Dwivedi, P. D. (2014). Interactive threats of nanoparticles to the biological system *Immunology Letters*, 158: 79 – 87.
- [3] Panyala, N.R., Pena-Mendez, E.M., Havel, J. (2008). Silver or silver nanoparticles: a hazardous threat to the environment and human health? *J. Applied Biomedicine*, 6: 117 – 129.
- [4] Asharani, P. V., Hande, M. P., Valiyaveetil, S. (2009a). Anti-proliferative activity of silver nanoparticles. *BMC Cell Biol.*, 10: 65.
- [5] Yang, W., Shen, C., Ji, Q., An, H., Wang, J., Liu, Q., Zhang, Z. (2009). Food storage material silver nanoparticles interfere with DNA replication fidelity and bind with DNA. *Nanotechnology*, 085102: 1 – 7.
- [6] Hubbs, A.F., Mercer, R.R., Benkovic, S.A., Harkema, J., Sriram, K., Schwegler- Berry, D., Goravanahally, M.P., Nurkiewicz, T.R., Castranova, V., Sargent, L.M. (2011). Nanotoxicology, a pathologist's perspective. *Toxicol. Pathol.*, 39: 301 – 324.
- [7] Chithrani, B. D. and Chan, W.C. (2007). Elucidating the mechanism of cellular uptake and removal of protein-coated gold nanoparticles of different sizes and shapes. *Nano Lett.*, 7: 1542 – 1550.
- [8] Dziendzikowska, K., Gromadzka-Ostrowska, J., Lankoff, A., Oczkowski, M., Krawczyńska, A., Chwastowska, J. et al. (2012). Time-dependent biodistribution and excretion of silver nanoparticles in male Wistar rats. *J. Appl. Toxicol.*, 32: 920 - 928.
- [9] [Song](#), M-F., [Li](#), Y-S., [Kasai](#), H., and [Kawai](#), K. (2012). Metal nanoparticle-induced micronuclei and oxidative DNA damage in mice. *J Clin. Biochem. Nutr.*, 50 (3): 211–216.
- [10] Garcia, T. X., Costac, G. M. J., Franc, L. R., Hofmann, M. C. (2014): Sub-acute intravenous administration of silver nanoparticles in male mice alters Leydig cell function and testosterone levels. *Reproductive Toxicology*, 45: 59– 70.
- [11] Asz, J., Asz, D., Moushey, R., Seigel, J., Mallory, S.B., Foglia, R.P. (2006). Treatment of toxic epidermal necrolysis in a pediatric patient with a nanocrystalline silver dressing. *J. Pediatr. Surg.*, 41: e 9–e 12.
- [12] Benn, T. M. and Westerhoff, P., (2008). Nanoparticle silver released into water from commercially available sock fabrics. *Environ. Sci. Technol.* 42, 4133–4139.
- [13] Ohashi, S., Saku, S., Yamamoto, K. (2004). Antibacterial activity of silver inorganic agent YDA filler. *J. Oral Rehabil.*, 31: 364 – 367.
- [14] Chou, W. L., Yu, D. G., Yang, M. C. (2005). The preparation and characterization of silverloading cellulose acetate hollow fiber membrane for water treatment. *Polym. Adv. Technol.*, 16: 600 – 607.
- [15] Xiao Y. and Gao, S. (2010). Use of IgY antibodies and semiconductor nanocrystal detection in cancer biomarker quantitation. *Biomarkers in medicine*, 4(2): 227-239.
- [16] Kim, Y. S., Song, M. Y., Park, J. D., Song, K.S., Ryu, H.R., Chung, Y. H., et al. (2010). Subchronic oral toxicity of silver nanoparticles. Part I. *Fibre Toxicol.*, 7: 20.
- [17] Park, E. J., Bae, E., Yi, J., Kim, Y., Choi, K., Lee, S. H. , et al. (2010). Repeated-dose toxicity and inflammatory responses in mice by oral administration of silver nanoparticles. *Environ Toxicol. Pharmacol.*, 30: 162 – 168.

- [18] Lee, Y., Kim, P., Yoon, J., Lee, B., Choi, K., Kil, K. H. et al. (2013). Serum kinetics, distribution and excretion of silver in rabbits following 28 days after a single intravenous injection of silver nanoparticles. *Nanotoxicology*, 7: 1120 – 1130.
- [19] Sharma, H. S., Hussain, S., Schlager, J., Ali, S. F., Sharma, A. (2010). Influence of nanoparticles on blood–brain barrier permeability and brain edema formation in rats. *Acta Neurochir Suppl.*, 106: 359 – 364.
- [20] Asharani, P. V., Low Kah Mun, G., Hande, M. P., Valiyaveetil, S. (2009b). Cytotoxicity and genotoxicity of silver nanoparticles in human cells. *ACS Nano.*, 3: 279 – 290.
- [21] Braydich-Stolle, L., Hussain, S., Schlager, J. J., Hofmann, M. C. (2005). In vitro cytotoxicity of nanoparticles in mammalian germline stem cells. *Toxicol Sci.*, 88:412 – 419.
- [22] Lankoff, A., Sandberg, W.J., Wegierek-Ciuk, A., Lisowska, H., Rafsnes, M., Sartowska, B., Schwarze, P.E., Meczynska-Wielgosz, S., Wojewodzka, M., Kruszewski, M. (2012). The effect of agglomeration state of silver and titanium dioxide nanoparticles on cellular response in HepG2 A549 and THP-1 cells. *Toxicology Letters*, 3: 197–213.
- [23] Greulich, C., Kittler, S., Epple, M., Muhr, G., Köller, M (2009). Studies on the biocompatibility and the interaction of silver nanoparticles with human mesenchymal stem cells (hMSCs). *Langenbecks Arch. Surg.*, 394: 495 – 502.
- [24] Bouwmeester, H., Poortman, J., Peters, R.J., Wijma, E., Kramer, E., Makama, S., Puspitaninganindita, K., Marvin, H.J., Peijnenburg, A.A., Hendriksen, P. J. (2011). Characterization of translocation of silver nanoparticles and effects on whole genome gene expression using an in vitro intestinal epithelium coculture model. *ACS Nano.*, 5: 4091 – 4103.
- [25] Park, M.V.D.Z., Neigh, A. M., Vermeulen, J. P., De La Fonteyne, L. J. J., Verharen, H. W., Briedé, J. J., et al. (2011). The effect of particle size on the cytotoxicity, inflammation, developmental toxicity and genotoxicity of silver nanoparticles. *Biomaterials*, 32: 9810 – 9817.
- [26] Ahamed, M., Posgai, R., Gorey, T.J., Nielsen, M., Hussain, S.M., Rowe, J.J. (2009). Silver nanoparticles induced heat shock protein 70, oxidative stress and apoptosis in *Drosophila melanogaster*. *Toxicol. Appl. Pharmacol.*, 242: 263 – 269.
- [27] Asharani, P. V., Wu, Y. L., Gong, Z., et al. (2008). Toxicity of silver nanoparticles in zebra fish models. *Nanotechnology*, 19 (25): 255102.
- [28] Laban, G., Nies, L.F., Turco, R.F., Bickham, J.W., Sepúlveda, M.S. (2010). The effects of silver nanoparticles on fathead minnow (*Pimephales promelas*) embryos. *Ecotoxicology* 19: 1 – 11.
- [29] Li, P.W., Kuo, T.H., Chang, J.H., Yeh, J.M., Chan, W.H., 2010. Induction of cytotoxicity and apoptosis in mouse blastocysts by silver nanoparticles. *Toxicology Letters*, 2: 82 –87.
- [30] Philbrook, N.A., Winn, L.M., Afrooz, A.R., Saleh, N.B., Walker, V.K. (2011). The effect of TiO₂ and Ag nanoparticles on reproduction and development of *Drosophila melanogaster* and CD-1 mice. *Toxicology and Applied Pharmacology*, 257: 429 – 436.
- [31] Gromadzka-Ostrowska, J., Dziendzikowska, K., Lankoff, A., Dobrzyńska, M., Instanes, C., Brunborg, G. et al. (2012): Silver Nanoparticles effects on epididymal sperm in rats. *Toxicol Lett.*, 214: 251 - 258.
- [32] Asare, N., Instanes, C.; Sandberg, W.J.; Refsnes, M.; Schwarze, P.; Kruszewski, M., Brunborg, G. (2012). Cytotoxic and genotoxic effects of silver nanoparticles in testicular cells. *Toxicology*, 291: 65 – 72.

- [33] Lim, D., Roh, J.-Y., Eom, H.-J., et al. (2012). Oxidative stress-related PMK-1/P38 MAPK activation as a mechanism for toxicity of silver nanoparticles to reproduction in the nematode *Caenorhabditis elegans*. *Environ. Toxicol. Chem.*, 31: 585 - 592.
- [34] Vernet, P., Aitken, R. J., Drevet, J. R. (2004). Antioxidant strategies in the epididymis. *Molecular and Cellular Endocrinology*, 216: 31 – 39.
- [35] El-Shenawy, N. S. (2009). Oxidative stress responses of rats exposed to Roundup and its Active ingredient glyphosate, *Environ. Toxicol. Pharmacol.*, 28: 379 – 385.
- [36] McShan, D., Ray, P. C., Yu, H. (2014). Molecular toxicity mechanism of nanosilver. *J. food and drug analysis*, xxx : 1 – 12.
- [37] Ahamed, M., Posgai, R., Gorey, T. J., Nielsen, M., Hussain, S. M., Rowe, J. J. (2010). Silver nanoparticles induced heat shock protein 70, oxidative stress and apoptosis in *Drosophila melanogaster*. *Toxicol Appl Pharmacol.*, 242: 263 – 269.
- [38] Ema, M., Kobayashi, N., Naya, M., Hanai, S., Nakanishi, J. (2010). Reproductive and developmental toxicity studies of manufactured nanomaterials. *Reprod. Toxicol.* 30: 343 – 352.
- [39] Pal, S., Tak, Y. K., Joon Myong Song, J. M. (2007). Does the Antibacterial Activity of Silver Nanoparticles Depend on the Shape of the Nanoparticle? A Study of the Gram-Negative Bacterium *Escherichia coli*. *Appl Environ Microbiol.*, 3(6): 1712–1720.
- [40] NIH (National Institute of Health) 1985. Guide for the Care and Use of Laboratory Animals, NIH Publication no. 85-23, National Research Council, Bethesda, Md, USA,
- [41] Rahman, M.F., Wang, J., Patterson, T. A., Saini, U. T., Robinson, B. L., Newport, G. D., Murdock, R. C., Schlager, J. J., Hussain, S. M., Ali, S. F. (2009). Expression of genes related to oxidative stress in the mouse brain after exposure to silver-25 nanoparticles *Toxicology Letters*, 187: 15–21.
- [42] Sagstad, A., Sanden, M., Krogaahl, A., Bakke-Mackillep, A. M., Frøystad, M., Hemre, G. I. (2008). Organs development, gene expression and health of Atlantic salmon (*Salmo Salar L.*) fed genetically modified soybeans compared to the near-isogenic non-modified parental line. *Aquacult Nutr.*, 14: 556 - 572.
- [43] D'Souza, R., Gill-Sharma, M. K., Pathak, S., Kedia, N., Kumar, R., Balasinar, N. (2005). Effect of high intratesticular estrogen on the seminiferous epithelium in adult male rats, *Mol. Cell Endocrinol.*, 241: 41 – 48.
- [44] Misra, H. P and Fridovich, I. (1972). The role of superoxide anion in the autoxidation of epinephrine and a simple assay for superoxide dismutase. *J. Biol. Chem.*, 247: 3170 - 3175.
- [45] Ohkawa, H., Ohishi, N., Yagi, K. (1979). Assay for lipid peroxides in animal tissues by thiobarbituric acid reaction. *Analytical Biochemistry*, 95: 351 – 358.
- [46] Narayana, K., D'Souza, U.J.A., Rao, K.P.S. (2002). Ribavirin induced sperm shape abnormalities in Wistar rat, *Mut. Res.*, 513: 193 – 196.
- [47] Tardif, S., Laforest, J. P., Comier, N., Bailey, J. L. (1999). The importance of porcine sperm parameters on fertility *in vivo*, *Theriogenology*, 52: 447– 459.
- [48] Linder, R. E., Klinefelter, G. R., Strader, L. F., Narotsky, M. G., Suarez, J. D., Roberts, N. L., Perreault, S. D. (1995). Dibromoacetic acid affects reproductive competence and sperm quality in the male rat. *Fund. Appl. Toxicol.*, 2825: 9 – 17.
- [49] Filler, R. (1993). Methods for evaluation of rats epididymal sperm morphology, in: R.E. Chapin, J.H. Heindel (Eds.), *Male Reproductive Toxicology*, Academic Press Inc., San Diego, CA: 334 – 343.

- [50] Erenpreiss, J., Bars, J., Lipatnikova, V., Erenpreisa, J., Zalkalns, J. (2001). Comparative study of cytochemical tests for sperm chromatin integrity. *J Androl.*, 22: 45 – 53.
- [51] Bancroft, J. D. and Gamble, M. (2007). *Theory and practice of histological techniques*. 6th ed. Churchill Livingstone: Elsevier Limited.
- [52] Robards, A. W. and Wilson, A. J. (1993). *Procedures in Electron Microscopy*, John Wiley & Sonns Ltd, Chichester. New York. Brisbane. Toronto. Singapore.
- [53] Shahare, B. and Yashpal, M. (2013). Toxic effects of repeated oral exposure of silver nanoparticles on small intestine mucosa of mice. *Toxicol. Mech. Methods* 23, 161–167. <http://dx.doi.org/10.3109/15376516.2013.764950> (Copyright (C) American Chemical Society (ACS). All Rights Reserved).
- [54] Bett, R. A.; Bradley, D. A.; Christenses, R. B.; Paulsen, C. A.; Bremner, W. J. and Matsumoto, A. M. (1996): Combined administration of Levonorgestrel and testosterone induces more rapid and effective suppression of spermatogenesis than testosterone alone: a promising male contraceptive approach. *Journal of Clinical Endocrinology Metabolism*, 81(2): 757 - 762.
- [55] Kruszewski, M., Brzoska, K., Brunborg, G., Asare, N., Dobrzynska, M., Duzinska, M., Fjellsbo, L.M., Georgantzopoulou, A., Gromadzka-Ostrowska, J., Gutleb, A.C. (2011). Toxicity of Silver Nanomaterials in Higher Eukaryotes. *Adv. Mol. Toxicol.*, 5: 179 – 259.
- [56] Aitken, R. J. and De Iuliis, G. N. (2010). On the possible origins of DNA damage in human spermatozoa. *Molecular Human Reproduction*, 16 (1): 3 – 13.
- [57] Pothuraju, R. and Kaul, G. (2013). Effect of silver nanoparticles on functionalities of Buffalo (*Bubalus Bubalis*) spermatozoa. *Adv. Sci. Eng. Med.*, 5: 91 - 95.
- [58] Mangelsdorf, I., Buschmann, J., Orthen, B. (2003). Some aspects relating to the evaluation of the effects of chemicals on male fertility. *Regul. Toxicol. Pharmacol.*, 37: 356 - 369.
- [59] Gupta, R. C. (2006). *Toxicology of organophosphates and carbamate compounds*, Elsevier Academic Press.
- [60] Mocan, T., Clichici, S., Agos_ton-Coldea, L., Mocan, L., Simon, S., Ilie, I.R., Biris, A.R., Mures, A. (2010). Implications of oxidative stress mechanisms in toxicity of nanoparticles (review). *Acta Physiol. Hung*, 97 (3): 247–255.
- [61] El-Tohamy, M. M. (2012). The mechanisms by which oxidative stress and free radical Damage produces male infertility, *Life Science J.*, 9(1): 674 – 688.
- [62] Chandra AK, Chatterjee A, Ghosh R, Sarkar M, Chaube SK. (2007). Chromium induced testicular impairment in relation to adrenocortical activities in adult albino rats. *Reprod Toxicol.*, 24 (3-4): 388 – 396.
- [63] Chandra, A. K.; Chatterjee, A.; Ghosh, R. and Sarkar, M. (2010): Vitamin E-supplementation protects chromium (VI)-induced spermatogenic and steroidogenic disorders in testicular tissues of rats. *Food and Chemical Toxicology*, 48 : 972 – 979.
- [64] Gerlach, T. and Aurich, J. E. (2000). Regulation of seasonal reproductive activity in the stallion, ram and hamster. *Animal Reproduction Science* 58 (3/4): 197 – 213.
- [65] O'Donnell, L., Robertson, K. M., Jones, M. E., Simpson, E.R. (2001). Estrogen and spermatogenesis. *Endocr. Rev.*, 22: 289 – 318.

- [66] Takeda, K., Suzuki, K. I., Ishihara, A., Kubo-Irie, M., Fujimoto, R., Tabata, M. et al. (2009). Nanoparticles transferred from pregnant mice to their offspring can damage the genital and cranial nerve systems. *J. Health Sci.*, 55: 95 - 102.
- [67] Hess, R.A. and Nakai, M. (2000). Histopathology of the male reproductive system induced by the fungicide benomyl. *Histology and Histopathology* 15, 207–224.
- [68] Yavasoglua, A., Ali Karaaslan, M., Uyanikgila, Y., Sayim, F., Atesa,U., Yavasoglub, N. U. K. (2008). Toxic affects of anatoxin-a on testes and sperm counts of male mice. *Experimental and Toxicologic Pathology*, 60: 391– 396.
- [69] Hofmann, M. C., Braydich-Stolle, L., Dettin, L., Johnson, E., Dym, M. (2005). Immortalization of mouse germ line stem cells. *Stem Cells*, 23: 200 – 210.
- [70] Liu, W., Wu, Y., Wang, C., Li, H.C., Wang, T., Liao, C.Y., Cui, L., Zhou, Q.F., Yan, B., Jiang, G.B., 2010. Impact of silver nanoparticles on human cells: effect of particle size. *Nanotoxicology*, 4: 319 – 330.
- [71] McAuliffe, M. and Perry, M. (2007). Are nanoparticles potential male reproductive toxicants? A literature review. *Nanotoxicol.*, 1(3): 204 - 210.
- [72] Toyama Y, Hosoi I, Ichikawa S, et al. (2001). Estradiol 3-benzoate affects spermatogenesis in the adult mouse. *Mol. Cell. Endocrinol.*, 178: 161 – 168.
- [73] Miresmaeili, S. M., Halvaei. I., Fesahat, F., Fallah, A., Nikonahad1, N. S., Taherinejad, M. (2013). Evaluating the role of silver nanoparticles on acrosomal reaction and spermatogenic cells in rat. *Iran J. Reprod. Med.*, 11 (5): 423 - 430.